Atmospheric Environment 304 (2023) 119776

Contents lists available at ScienceDirect

Atmospheric Environment

journal homepage: www.elsevier.com/locate/atmosenv

Rapid increase in tropospheric ozone over Southeast Asia attributed to changes in precursor emission source regions and sectors

Su Li [a], Yang Yang [a,*], Hailong Wang [b], Pengwei Li [a], Ke Li [a], Lili Ren [a], Pinya Wang [a], Baojie Li [a], Yuhao Mao [a], Hong Liao [a]

[a] Joint International Research Laboratory of Climate and Environment Change (ILCEC), Jiangsu Key Laboratory of Atmospheric Environment Monitoring and Pollution Control, Jiangsu Collaborative Innovation Center of Atmospheric Environment and Equipment Technology, School of Environmental Science and Engineering, Nanjing University of Information Science and Technology, Nanjing, Jiangsu, China

[b] Atmospheric Sciences and Global Change Division, Pacific Northwest National Laboratory, Richland, WA, USA

HIGHLIGHTS

- Source apportionments of tropospheric ozone in Southeast Asia from 1990 to 2019 are quantified with a tagging technique.
- Significant increase in local NO_x emissions is the reason for the increase in tropospheric ozone in Southeast Asia.
- NO_x emissions from ground transportation and international shipping explain the rapid rise in ozone concentrations.
- Increasing anthropogenic NO_x emissions enhance the efficiency of ozone production by VOCs.

GRAPHICAL ABSTRACT

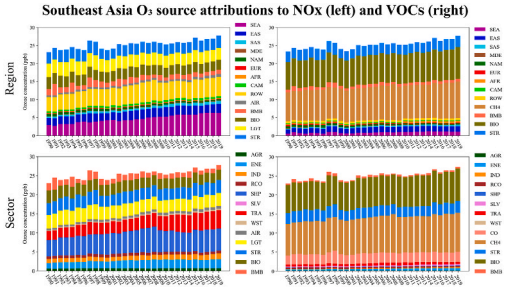

ABSTRACT

Observations indicate that tropospheric ozone (O_3) concentrations over Southeast Asia have been increasing rapidly since the 1990s. Here, we quantify source contributions from geographical regions and emission sectors of the two distinct types of O_3 precursors, i.e., nitrogen oxides (NO_x) and volatile organic compounds (VOCs), to the increase in tropospheric O_3 in Southeast Asia during 1990–2019 using an O_3 source tagging technique implemented in a global chemistry-climate model. The results show that although local anthropogenic emission of NO_x in Southeast Asia only contributes 18% of the annual averaged near-surface O_3 concentration, the increase in local NO_x emission dominates the increasing trend of O_3 concentration in Southeast Asia, accounting for 107% of the regional averaged trend of 1.07 ppb decade^{-1}. Increases in NO_x emissions from East Asia and South Asia explain 29% of the increasing trend, but 9% is offset by the emission reduction in North America. The vertical O_3 trends in the troposphere contributed by individual source regions are consistent with those near the surface. Ground transportation is responsible for 79% of the rapid O_3 increase, followed by 39% contribution from international shipping. Because an increase in anthropogenic NO_x emissions enhances the O_3 production efficiency by VOCs, the increase in O_3 concentrations in Southeast Asia is thereby largely contributed by methane and biogenic VOCs.

1. Introduction

Tropospheric ozone (O_3) is an important greenhouse gas that can produce positive radiative forcing at the top of the atmosphere. It is also one of the major secondary air pollutants that damages human health by causing respiratory disease, harms vegetation, and prevents carbon

* Corresponding author.
E-mail address: yang.yang@nuist.edu.cn (Y. Yang).

https://doi.org/10.1016/j.atmosenv.2023.119776
Received 24 November 2022; Received in revised form 22 March 2023; Accepted 10 April 2023
Available online 11 April 2023

uptake by the biosphere (Sitch et al., 2007). Tropospheric O_3 is mainly produced through photochemical reactions of O_3 precursors such as nitrogen oxides (NO_x), volatile organic compounds (VOCs), and carbon monoxide (CO) in the presence of sunlight. It also comes from the stratosphere-troposphere exchange. Given the relative long lifetime of O_3 in the free troposphere, it can be transported by atmospheric circulation to distant regions and has a far-reaching effect on air quality (Jacob et al., 1999).

Since the 1970s, the implementation of O_3 control measures has resulted in a significant decrease in O_3 concentrations observed at most stations worldwide (Schultz et al., 2017), especially over North America and Europe where anthropogenic emissions of NO_x and VOCs were effectively controlled (Sicard et al., 2020; Zhang et al., 2019). In the last few decades, due to the continued growth in energy consumption and infrastructure development, it is well documented that emissions in Asia have increased dramatically, especially in East Asia and South Asia (Kurokawa et al., 2013). Although NO_x and CO emissions have been largely reduced in China owing to clean air actions since 2010, non-methane VOCs (NMVOCs) emissions are still increasing (Zheng et al., 2018), leading to the elevated O_3 levels in China (Lu et al., 2020).

Based on surface observations (Cooper et al., 2020) and aircraft measurements (Gaudel et al., 2020), the latest IPCC AR6 (Sixth Assessment Report of the Intergovernmental Panel on Climate Change) reported that Southeast Asia had the largest increasing trend of O_3 concentration by 4–6 parts per billion (ppb) per decade since 1994, rather than East Asia or South Asia (Szopa et al., 2021). The rapid increase in O_3 in Southeast Asia was also found in many other studies (Chang et al., 2017; Gaudel et al., 2018; Ziemke et al., 2019; Ahamad et al., 2020; Wang et al., 2022). Zhang et al. (2016) indicated that it was related to equatorward redistribution of anthropogenic emissions of O_3 precursors from developed to developing regions since 1980. Due to the intense sunlight, frequent deep convection, high temperature, and strong O_3 sensitivity to emissions at low latitudes, the increase in NO_x emissions has led to the unexpected increase in O_3 concentrations in Southeast Asia (Zhang et al., 2021). However, it is still unknown which emission sectors or regions are responsible for the O_3 increase in Southeast Asia. Wang et al. (2022) suggested that the growing anthropogenic emissions dominated the O_3 increase over Peninsular Southeast Asia, but they did not quantitatively attribute the O_3 increase to individual source regions.

Source apportionment of air pollutants to emitting regions and sectors is useful to policymaking of emission control measures (Ren et al., 2020, 2021; Yang et al., 2017, 2018, 2021). Fiore et al. (2009) estimated the impact of source regions on tropospheric O_3 in receptor regions by comparing the results between reference simulation and sensitivity simulations, in which a small perturbation (e.g., 20% reduction) is applied to anthropogenic O_3 precursors emitted from various source regions. This approach was also adopted in several studies (e.g., Fiore et al., 2002; Auvray and Bey, 2005; Guerova et al., 2057). Since O_3 production has a strong nonlinear relationship with its precursors, simply perturbing or turning off anthropogenic emissions from a given region for a particular O_3 precursor can only characterize the response of O_3 to an emission change, but cannot accurately quantify the contributions of precursors from various emitting regions and sectors to the total O_3 concentrations.

Recently, many studies used tagging methods to apportion O_3 to different sources. Sudo and Akimoto (2007) applied O_3 tagging method in a global chemical transport model to study the long-range transport of tropospheric O_3 from various source regions, but they only tagged O_3 produced from source regions rather than its precursors. In Emmons et al. (2012), O_3 tagging was implemented in the Model for Ozone and Related chemical Tracers (MOZART-4) by using artificial tracers of NO and its oxidation products, without considering VOCs. Some studies considered both NO_x and VOCs for O_3 tagging but simply gave equal weight to the two distinct types of O_3 precursors (Grewe et al., 2017; Guo et al., 2017). In the O_3 tagging method used by Butler et al. (2018, 2020), earlier work of Emmons et al. (2012) was extended and improved by attributing tropospheric O_3 to both NO_x and VOCs emissions, as well as to transport from the stratosphere, in two separate simulations.

Previous studies revealed an important role of precursor emissions from Southeast Asia in the global tropospheric O_3. However, exact sources leading to the recent strong O_3 increase in Southeast Asia have not been identified. In this paper, by adopting the O_3 tagging technique described by Butler et al. (2018), we simulate tropospheric O_3 from 1990 to 2019 in a global chemistry-climate model and quantify contributions to O_3 concentrations in Southeast Asia from different emitting regions and sectors of O_3 precursors. Sect. 2 describes the model configuration, tagging method, and experimental design. Sect. 3 shows results on the quantified trends of source contributions of emitting regions and sectors to O_3 concentrations in Southeast Asia. Sect. 4 summarizes the main conclusions.

2. Methodology

2.1. Model description

The Community Atmosphere Model version 4 with chemistry (CAM4-chem) (Lamarque et al., 2012), which is the atmospheric chemistry component of CESM (the Community Earth System Model) version 1.2.2, is utilized in this study to simulate tropospheric O_3. The model with the component setup of "FMOZ" is run at a spatial resolution of 1.9° (latitude) × 2.5° (longitude) with 26 vertical layers. This configuration applies atmospheric chemistry mechanism expanded from the Model for Ozone and Related chemical Tracers version 4 (MOZART-4) (Emmons et al., 2010). Wind fields are nudged in this study toward the MERRA-2 reanalysis (Gelaro et al., 2017) to capture the observed atmospheric circulations. A comprehensive assessment of the model's performance in simulating global tropospheric concentrations of O_3 and precursors has been carried out by Tilmes et al. (2015), which showed that the observed tropospheric O_3 over the tropics and Northern Hemisphere could be well reproduced by the model.

2.2. Ozone source tagging technique

The O_3 source tagging technique recently implemented in CESM1.2.2 (Butler et al., 2018) is able to provide a separate attribution of tropospheric O_3 to emissions of its precursors from individual sources, as well as the O_3 transported from the stratosphere. Attributing tropospheric O_3 to its precursors requires two parallel model runs, with NO_x and VOCs tagged, respectively. More information of the O_3 tagging technique refers to Butler et al. (2018).

Source-receptor relationships of tropospheric O_3 are quantified in this study by geographical regions and emitting sectors. Southeast Asia (12°S–20°N, 92°E–162°E) is the receptor region of interest. Anthropogenic emissions of NO_x and NMVOCs from 9 geographical regions are

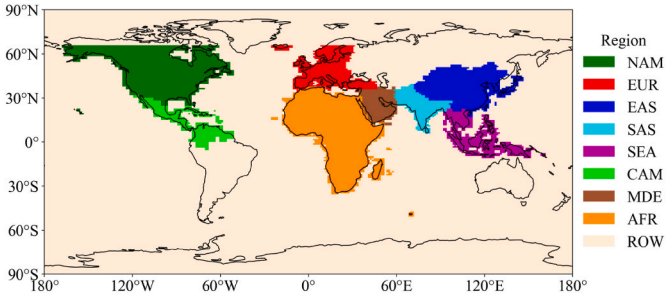

Fig. 1. Source regions defined for O_3 tagging, including North America (NAM), Europe (EUR), East Asia (EAS), South Asia (SAS), Southeast Asia (SEA), Central America (CAM), the Middle East (MDE), Africa (AFR), and the rest of the world (ROW).

tagged (Fig. 1), including Europe (EUR), North America (NAM), Central America (CAM), Middle East (MDE), Southeast Asia (SEA), South Asia (SAS), East Asia (EAS), Africa (AFR), and the rest of the World (ROW), in two parallel simulations (NO_x-tagging and VOC-tagging). Natural sources, including chemical production in the stratosphere (STR), biomass burning emissions (BMB), biogenic emissions (BIO), lightning production (LGT) and extra chemical production (XTR) are also tagged. Additional tags for methane (CH_4) and CO are applied in the VOC-tagging simulation.

Another set of simulations partitioning O_3 into individual source sectors of NO_x and VOCs are also performed. Anthropogenic emissions from different sectors, including agriculture (AGR), energy transformation and extraction (ENE), industrial combustion and processes (IND), residential, commercial and other (RCO), ground transportation (TRA), waste disposal and handling (WST), international shipping (SHP), and solvents (SLV), are separately tagged for NO_x and NMVOCs in the NO_x-tagging and VOCs-tagging simulations, respectively. Natural sources and CH_4 are separately tagged in this set of simulations.

2.3. Emissions of ozone precursors

The global historical anthropogenic emissions of NO_x, CO, and NMVOCs during 1990–2019 are from the Community Emissions Data System (CEDS) version 20210205 (Hoesly et al., 2018). Biomass burning emissions over 1990–2014 are derived from the historical inventory (van Marle et al., 2017), and the remaining years (2015–2019) are from SSP2-4.5 scenario (O'Neill et al., 2016) of the CMIP6 (Coupled Model Intercomparison Project Phase 6). NO_x and NMVOCs emissions from biogenic sources are specified in Tilmes et al. (2015) and held at present-day climatological levels. NO_x emissions from lightning are estimated according to Price et al. (1997). CH_4 concentrations are kept at a global mean level of 1760 ppb.

Fig. 2 presents the time series of NO_x and NMVOCs emissions from individual sectors over Southeast Asia during 1990–2019. In general, the NO_x emissions increased rapidly from 1990 to about 2015, owing to the emission increases from ground transportation, international shipping and energy sectors, and then slightly declined. NMVOCs emissions also show moderate growth during 1990–2019, primarily due to the emission increases from ground transportation and energy sectors. The biomass burning emissions of NMVOCs display a large interannual variability, which exert high emissions in certain years (e.g., 1991 and 1997).

2.4. Experimental design

Four groups of experiments are performed in this study, each of which has two parallel simulations with NOx-tagging and VOCs-tagging, respectively. In two baseline groups, emissions from geographical source regions and individual emission sectors are tagged separately. The two baseline groups (BASE) are driven by the time-varying emissions of O_3 precursors and wind fields, which are primarily used to quantify source contributions to increases in O_3 levels in Southeast Asia unless stated otherwise. The other two groups of experiments (MET) have the same model configuration as BASE, except that anthropogenic emissions are kept at the level of year 2019. The relative influences of changes in anthropogenic emissions and large-scale circulations on O_3 trends can be derived by comparing BASE and MET simulations. All simulations are conducted from 1990 to 2019 following a two-year model spin-up.

3. Results

3.1. Source apportionment of tropospheric ozone in Southeast Asia

Based on the unique global O_3 tagging technique, modeled near-surface O_3 concentrations in Southeast Asia can be quantitatively attributed to the precursor NO_x and VOCs emitted from both local Southeast Asian sources and remote source regions, as well as specific source sectors. Fig. 3 illustrates the relative contributions of NO_x and VOCs emissions from the major tagged source regions and sectors to the annual mean near-surface O_3 concentrations in Southeast Asia averaged over 1990–2019.

In the NO_x-tagging experiments, Southeast Asia local anthropogenic emission of NO_x only explains 18% of the annual mean near-surface O_3 in Southeast Asia, while long-range transport of O_3 generated by anthropogenic NO_x emissions from regions outside Southeast Asia and O_3 production from natural sources dominate near-surface O_3 in Southeast Asia. Anthropogenic emission of NO_x from the rest of the world and East Asia has a contribution of 19% and 9%, respectively (Fig. 3a). Among the emission sectors, international shipping emission of NO_x has the largest contribution to the near-surface O_3 concentration in Southeast Asia (22%) (Fig. 3c), which also explains the large contribution of emissions from the rest of the world. Ground transportation and energy related emissions contribute 14% and 8% to the O_3 in Southeast Asia, respectively. Natural sources such as lightning production and those from the stratosphere, biogenic emission and biomass burning emission of NO_x account for 14%, 12%, 11% and 6% of the near-surface O_3 in Southeast Asia, respectively.

In the VOCs-tagging, CH_4 and biogenic NMVOCs (BVOCs) are the major sources of annual mean near-surface O_3 concentration in Southeast Asia, each contributing about one-third of the O_3 concentration. Anthropogenic NMVOCs only contributes about 10% of O_3 concentration in Southeast Asia (Fig. 3b and d).

Fig. 4 shows the vertical profile of contributions from individual source regions and sectors to annual mean tropospheric O_3 concentrations in Southeast Asia. In the NO_x-tagging experiments, local emissions and ROW emissions are the primary sources of tropospheric O_3 in Southeast Asia below 500 hPa. Above 500 hPa, stratospheric O_3 intrusion and emissions from lightning activity account for the majority of O_3 in Southeast Asia. Anthropogenic emissions of NO_x from East Asia and

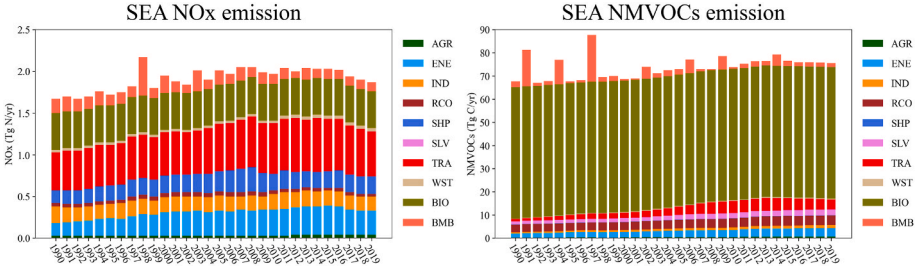

Fig. 2. Time series of NO_x (Tg N yr^{-1}) and NMVOCs (Tg C yr^{-1}) emissions from individual sectors over Southeast Asia during 1990–2019, including agriculture (AGR), energy transformation and extraction (ENE), industrial combustion and processes (IND), residential, commercial and other (RCO), international shipping (SHP), solvents production and application (SLV), ground transportation (TRA), waste disposal and handling (WST), biogenic emissions (BIO), and biomass burning (BMB).

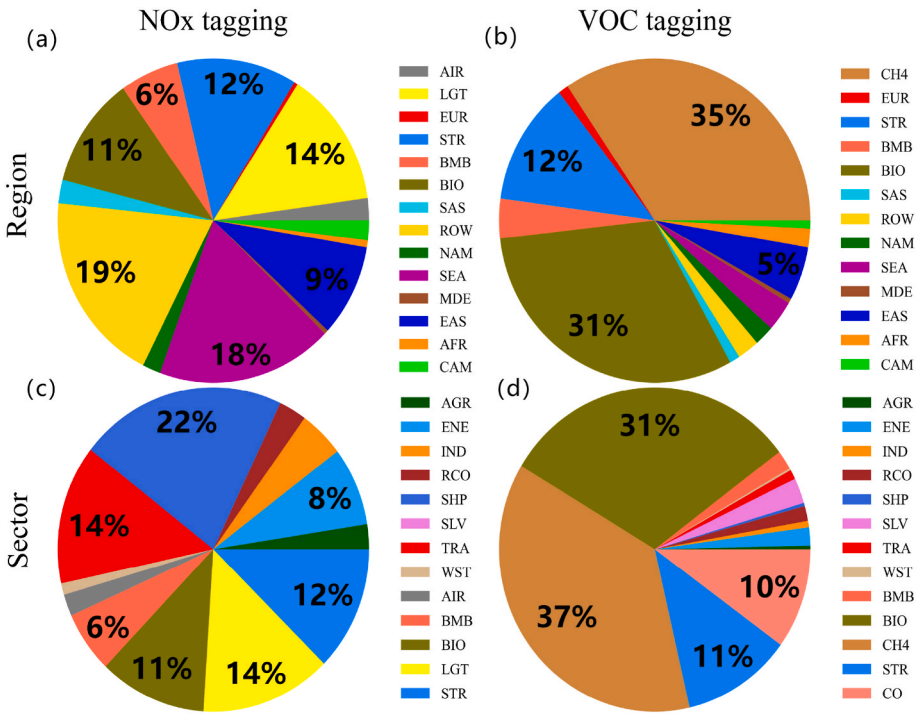

Fig. 3. Relative contributions (%) to annual mean near-surface O_3 in Southeast Asia averaged over 1990–2019 by (a, c) NO_x and (b, d) VOCs emissions from individual source regions (top) and sectors (bottom). Source regions include the nine regions defined in Fig. 1 for anthropogenic emissions, as well as global BMB, BIO, aircraft (AIR), lightning (LGT), stratosphere (STR), and CH_4. Emission sectors include AGR, ENE, IND, RCO, SHP, SLV, TRA, WST, BMB, BIO, AIR, LGT, STR, as well as those produced by CO and CH_4. Values larger than 5% are marked.

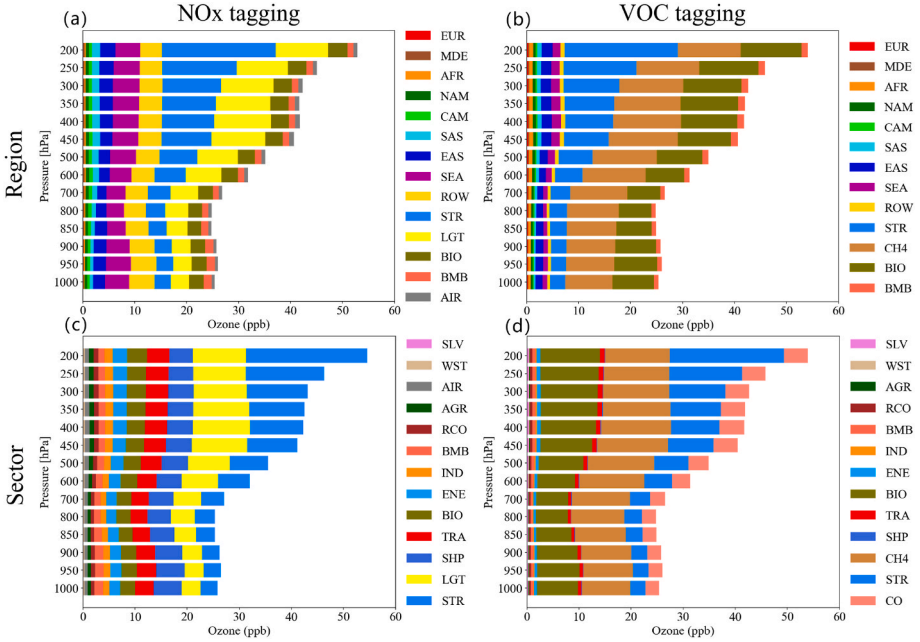

Fig. 4. Annual mean vertical profile of tropospheric O_3 concentrations (ppb) over Southeast Asia contributed by (a, c) NO_x and (b, d) VOCs emitted from individual source regions (top) and sectors (bottom) during 1990–2019.

South Asia also contribute considerably to Southeast Asian O_3 at all altitudes by 4–5 parts per billion (ppb). International shipping and ground transportation are the two main contributors among all anthropogenic sectors of NO_x across the troposphere. In the VOCs-tagging simulations, BVOCs and CH_4 together are responsible for more than half of the O_3 from the surface to 300 hPa and the stratospheric contribution increases with height in the troposphere.

3.2. Ozone trend contributed by individual source regions

The model simulations (both NO_x-tagging and VOCs-tagging) show that near-surface O_3 concentrations in Southeast Asia have been increasing since 1990 (Fig. 5), with the most significant increase of 4–5 ppb decade^{-1} over the maritime Southeast Asia (Fig. 6a), which is consistent with the observations. However, the observation shows a strong increase in O_3 concentrations by 4–5 ppb decade^{-1} around the mainland Southeast Asia, while the model only predicts 2–3 ppb decade^{-1} increase in this region. With time-varying emissions considered, all

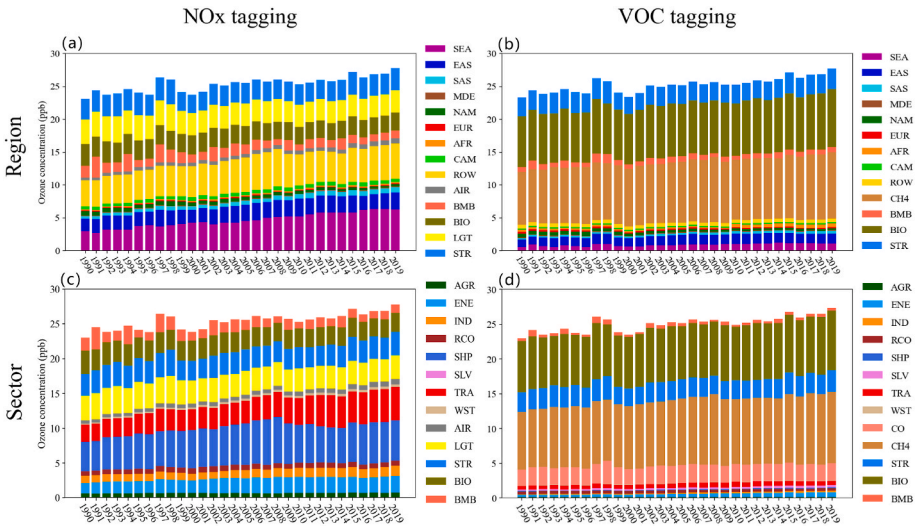

Fig. 5. Time series of near-surface O_3 concentrations (ppb) averaged over Southeast Asia contributed by NOx (a, c) and VOCs (b, d) emitted from individual source regions (top) and sectors (bottom) during 1990–2019.

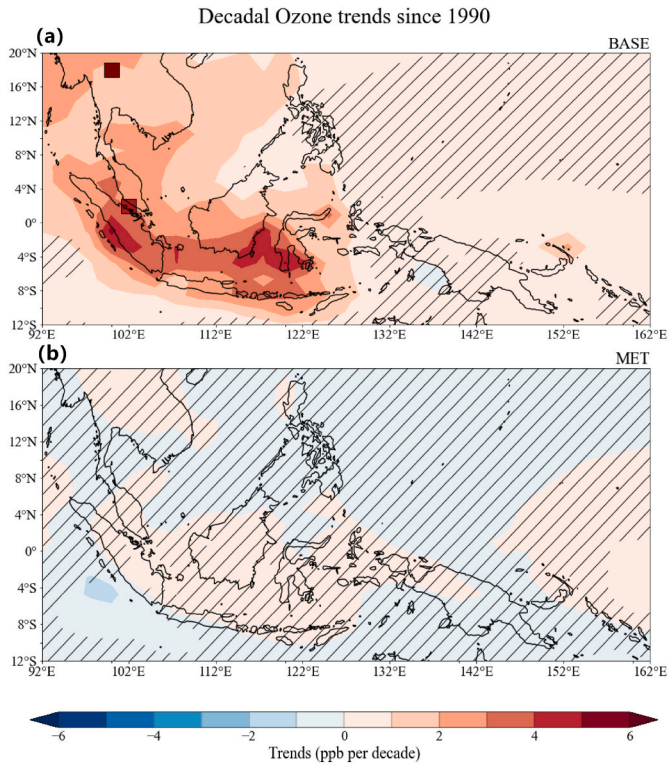

Fig. 6. Linear trends (ppb decade^{-1}) of simulated (contours) annual mean near-surface O_3 concentrations during 1990–2019 from (a) BASE and (b) MET experiments. Observed trends of O_3 concentrations during 1994–2016 at two regions from Gaudel et al. (2020) are also shown in (a) as color-filled boxes. Areas without hatches indicate statistical significance with 95% confidence.

regions in Southeast Asia show an increasing trend of 2–5 ppb decade^{-1} in the BASE experiments, with a regional averaged trend of 1.07 ppb decade^{-1}. In the MET experiments with emissions fixed at year-2019 level, the O_3 trends decrease to those within ±1 ppb decade^{-1} and are statistically insignificant across Southeast Asia, suggesting that the emission changes dominate the O_3 trends over Southeast Asia during 1990–2019 in the BASE experiments.

Throughout the troposphere, the simulated O_3 column burden also shows an increasing trend of 1–3 DU decade^{-1} (Fig. 7a) over Southeast Asia averaged over 2004–2019, which is lower than satellite retrievals during 2005–2020 (2–4 DU decade^{-1}) (Fig. 7b). The bias in the modeled trends of O_3 burden is partly because the model underestimates the annual O_3 burden in the mainland Southeast Asia but overestimates it over Maritime Continents, comparing to the satellite retrievals (Fig. 7c and d). In addition, CEDS emission inventory has been reported to underestimate NO_x emission trends over the mainland Southeast Asia but overestimate the emission trends over Maritime Continents in the recent decade (Wang et al., 2022), leading to the low bias of O_3 trends over the mainland Southeast Asia and the downwind areas.

Fig. 8 decomposes the modeled trend of near-surface O_3 concentrations in Southeast Asia into contributions from individual source regions. Although local anthropogenic NO_x emissions only account for about one-fifth of the annual O_3 concentration, it is responsible for the decadal trend of the O_3 concentrations in Southeast Asia during 1990–2019, contributing to 1.15 ppb decade^{-1} (107% relative to the total trend) of the O_3 trend. The increase in local NO_x is in accordance with satellite retrievals (Georgoulias et al., 2019). Anthropogenic NO_x emissions from the rest of the world account for 0.37 ppb decade^{-1} (35%) of the trend, followed by 0.19 and 0.12 ppb decade^{-1} (18% and 11%) due to NO_x emissions from East Asia and South Asia, respectively, partly offset by −0.11 ppb decade^{-1} (−10%) due to an emission decline in North America. Specifically, from 1990 to 2019, anthropogenic NO_x emissions increased by 65% and 161% in East Asia and South Asia, respectively, and decreased by 56% in North America according to the CEDS inventory. Increased aircraft emissions lead to an O_3 increase of 0.09 ppb decade^{-1} (8%). Although natural sources are kept unchanged during the simulation, their changes tend to reduce near-surface O_3 concentration, associated with the weakened O_3 production efficiency by NO_x with increases in anthropogenic NO_x emissions.

For VOC-tagging, as the increases in anthropogenic NO_x emissions, the O_3 production efficiency by VOCs increases, leading to the large increasing O_3 trends of 0.58 and 0.33 ppb decade^{-1} (54% and 31%) in Southeast Asia contributed by CH_4 and BVOCs, respectively. Anthropogenic NMVOCs emissions from Southeast Asia, East Asia, Africa and South Asia contribute to the increasing O_3 trend by 0.17, 0.09, 0.06 and 0.05 ppb decade^{-1} (16%, 8%, 6% and 5%), respectively, while emission reductions in North America and Europe dampen the trend by 0.10 and 0.06 ppb decade^{-1} (9% and 6%), respectively, during 1990–2019.

The difference in source region contributions to the vertical profile of tropospheric O_3 concentrations over Southeast Asia between 2015–2019 and 1990–1994 (Fig. 9) shows that the largest increasing trend of O_3 concentration is around 450 hPa, related to the tropical convection

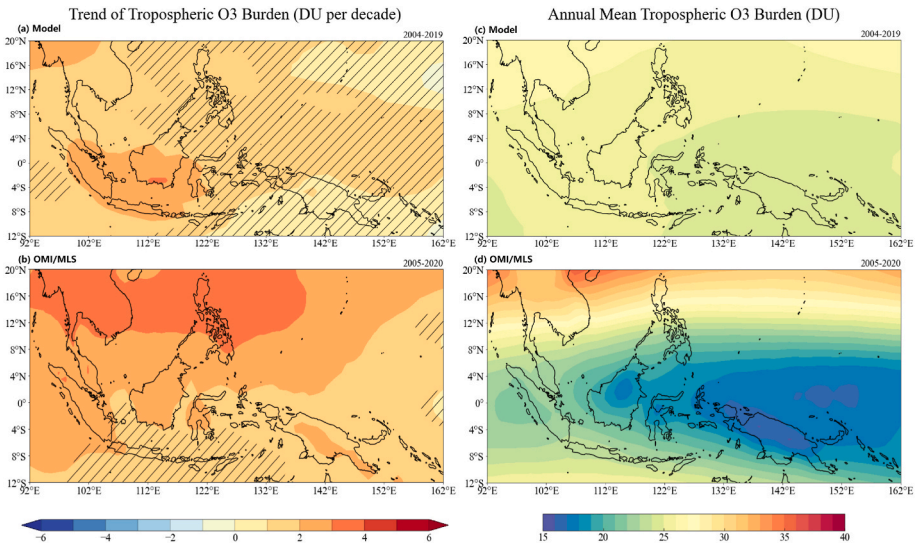

Fig. 7. (a, b) Linear trends (DU decade^{-1}) and (c, d) 16-year average (DU) of annual mean tropospheric O_3 burden from the BASE simulation (2004–2019, top) and (b) OMI/MLS satellite retrievals (2005–2020, bottom). Areas without hatches indicate statistical significance with 95% confidence.

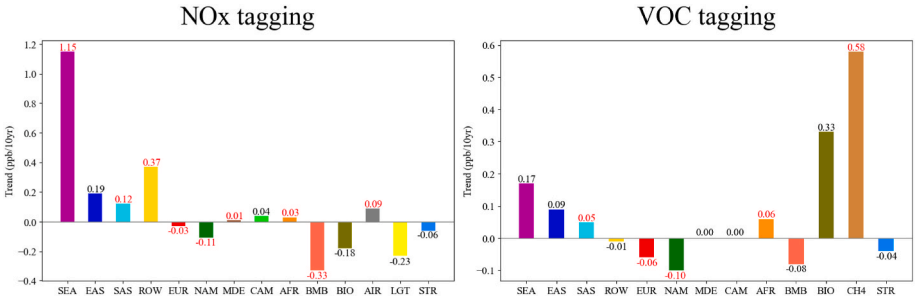

Fig. 8. Linear trends (ppb decade^{-1}) of near-surface O_3 concentrations in Southeast Asia contributed by NO_x (left) and VOCs (right) emitted from individual source regions. The trends marked with red color numbers indicate statistical significance with 95% confidence.

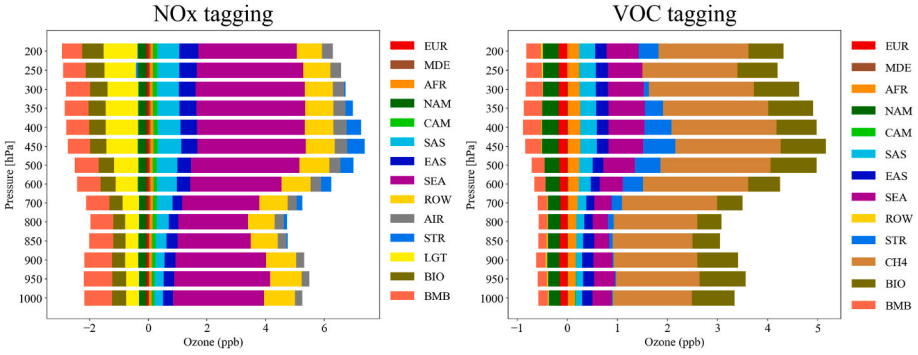

Fig. 9. Changes in annual mean vertical profile of tropospheric O_3 concentrations over Southeast Asia between 1990–1994 and 2015–2019 contributed by the NO_x (left) and VOCs (right) emitted from individual source regions.

lifting the emitted O_3 precursors to higher altitudes and more intense sunlight there. Southeast Asian local NO_x emissions contribute the largest portion of the O_3 increase throughout the troposphere, followed by the rest of the world, South Asia, and East Asia. The contributions of anthropogenic NO_x emissions from Europe and North America to tropospheric O_3 in Southeast Asia decrease at all altitudes due to their effective emission reduction. The contributions of lightning, biogenic emissions, and biomass burning emissions also decrease throughout the troposphere. CH_4 is the largest contributor to the increase in tropospheric O_3 in Southeast Asia among the VOC tags, followed by BVOCs emissions, due to the increases in NO_x emissions and the enhanced O_3 production efficiency by VOCs.

3.3. Ozone trend contributed by emission sectors

Time series of annual near-surface O_3 concentrations averaged over Southeast Asia is shown in Fig. 5 and trends of O_3 concentrations contributed by individual emitting sectors during 1990–2019 are shown in Fig. 10. During the analyzed period, anthropogenic NO_x emission from ground transportation has the largest contribution of 0.84 ppb

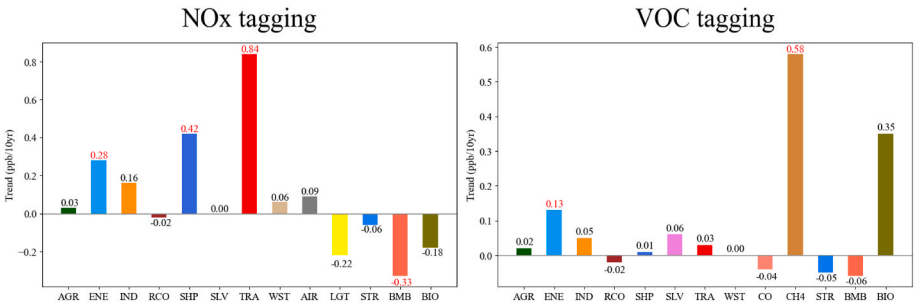

Fig. 10. Linear trends (ppb decade^{-1}) of near-surface O_3 concentrations over Southeast Asia contributed by NO_x (left) and VOCs (right) emitted from individual sectors. The trends marked with red color numbers indicate statistical significance with 95% confidence.

decade^{-1} (79%) to the increasing O_3 trend among all sectors, which is due to the large increase in NO_x emission from this sector (Fig. 2). International shipping (0.42 ppb decade^{-1} or 39%), energy (0.28 ppb decade^{-1} or 26%) and industry (0.16 ppb decade^{-1} or 15%) sectors also contribute to the O_3 increase in Southeast Asia, consistent with the emission changes during this time period. Decrease in biomass burning emission together with the weakened O_3 production efficiency by NO_x accounts for a decrease of −0.33 ppb decade^{-1} (−31%) in O_3 concentration.

When the O_3 trend is attributed to VOCs, CH_4 and BVOCs contribute the most to the increasing O_3 trend in Southeast Asia, resulting from their dominant roles in O_3 production and enhanced O_3 production efficiency by VOCs. The increase in NMVOCs emission from energy sector (Fig. 2) is responsible for 0.13 ppb decade^{-1} (12%) of the O_3 increase. Although NMVOCs emission from ground transportation increased the largest among all sectors, the O_3 produced by this sector only shows a weak increase in Southeast Asia during 1990–2019, possibly owing to the non-linear response of O_3 production to its precursor emissions in sub-regions of Southeast Asia, which deserves further exploration with finer model resolution.

4. Conclusions and discussions

Tropospheric O_3 concentrations in Southeast Asia have been increasing rapidly since 1990s, but quantitative attributions of the O_3 increase in Southeast Asia to different source regions and sectors of its precursor emissions lack a comprehensive investigation. In this study, using a global chemistry-climate model with an explicit O_3 source tagging technique, we investigate the long-term trends and source apportionments of tropospheric O_3 concentrations in Southeast Asia during 1990–2019. The O_3 trends in Southeast Asia over 1990–2019 were found to be dominated by changes in anthropogenic emissions rather than in large-scale atmospheric circulation.

Overall, the annual tropospheric O_3 concentrations in Southeast Asia are dominated by the long-range transport of O_3 generated by anthropogenic NO_x emissions from regions outside Southeast Asia and O_3 from natural sources, while local anthropogenic NO_x emissions only contribute 18% of annual average near-surface O_3 in Southeast Asia. However, local NO_x emissions account for 107% of the simulated near-surface O_3 increasing trend of 1.07 ppb decade^{-1} averaged over Southeast Asia, which is due to a large increase in local anthropogenic NO_x emissions during 1990–2019. Increases in anthropogenic NO_x emissions from East Asia and South Asia explain 29% of the O_3 increasing trend, but 10% of the trend is offset by the NO_x emission reduction in North America. The vertical O_3 trends in the troposphere contributed by individual source regions are consistent with those near the surface. The increase in NO_x emissions from ground transportation is responsible for 79% of the near-surface O_3 increasing trend in Southeast Asia, followed by 39% contribution from the more frequent international shipping activities. A decrease in biomass burning NO_x emission reduces the O_3 increasing trend by 31%.

Anthropogenic NMVOCs emissions account for 10% of the averaged near-surface O_3 concentration in Southeast Asia, while CH_4 and BVOCs contribute 37% and 31%, respectively. CH_4 and BVOCs are also the largest contributors (54% and 31%) to the increase in near-surface O_3 concentrations in Southeast Asia, which is because the increase in anthropogenic NO_x emissions enhances the O_3 production efficiency of VOCs. Anthropogenic NMVOCs emissions from Southeast Asia, East Asia, Africa and South Asia contribute to the O_3 increasing trends by 16%, 8%, 6% and 5%, respectively, while emission reductions in North America and Europe dampen the increasing trends by 9% and 6% during 1990–2019.

This study quantitatively examined the contributions of major source regions and sectors of O_3 precursor emissions to tropospheric O_3 concentrations in Southeast Asia based on the state-of-the-art O_3 tagging technique implemented in a global chemistry-climate model. The results are expected to provide new insights into the mitigation of O_3 pollution in Southeast Asia from perspectives of local sources and intercontinental transport. It should be noted that the model underestimates the O_3 trends in terms of both near-surface concentration and column burden in the mainland Southeast Asia, which is likely related to biases in emission inventory (Wang et al., 2022). If the O_3 trends are accurately simulated by the model, the source contributions from anthropogenic NO_x emissions would be larger than estimated here. Additionally, due to the lack of long-term observations, the results are presented with model simulations together with limited observational and satellite data. More observations are required to support the modeling results in the future.

CRediT authorship contribution statement

Su Li: Conceptualization, Data curation, Formal analysis, Investigation, Methodology, Software, Visualization, Writing – original draft. **Yang Yang:** Conceptualization, Data curation, Formal analysis, Project administration, Supervision, Writing – review & editing. **Hailong Wang:** Formal analysis, Writing – review & editing. **Pengwei Li:** Data curation. **Ke Li:** Writing – review & editing. **Lili Ren:** Formal analysis. **Pinya Wang:** Formal analysis. **Baojie Li:** Formal analysis. **Yuhao Mao:** Formal analysis. **Hong Liao:** Formal analysis.

Declaration of competing interest

The authors declare that they have no known competing financial interests or personal relationships that could have appeared to influence the work reported in this paper.

Data availability

I have shared the link to my data.

Acknowledgments

This study was supported by the National Key Research and

Development Program of China (grant 2020YFA0607803), the National Natural Science Foundation of China (grant 42293323), Jiangsu Science Fund for Distinguished Young Scholars (grant BK20211541) and Jiangsu Science Fund for Carbon Neutrality (grant BK20220031). HW acknowledges the support by the U.S. Department of Energy (DOE), Office of Science, Office of Biological and Environmental Research (BER), as part of the Earth and Environmental System Modeling program. The Pacific Northwest National Laboratory (PNNL) is operated for DOE by the Battelle Memorial Institute under contract DE-AC05-76RLO1830. The authors thank Prof. Tim Butler for his very helpful input regarding the implementation of ozone tagging technique.

References

Ahamad, F., Griffiths, P.T., Latif, M.T., Juneng, L., Xiang, C.J., 2020. Ozone trends from two decades of ground level observation in Malaysia. Atmosphere 11, 755. https://doi.org/10.3390/atmos11070755.

Auvray, M., Bey, I., 2005. Long-range transport to Europe: seasonal variations and implications for the European ozone budget. J. Geophys. Res. 110, D11303 https://doi.org/10.1029/2004JD005503.

Butler, T., Lupascu, A., Coates, J., Zhu, S., 2018. TOAST 1.0: tropospheric ozone attribution of sources with tagging for CESM 1.2.2, geosci. Model Dev 11, 2825–2840. https://doi.org/10.5194/gmd-11-2825-2018.

Butler, T., Lupascu, A., Nalam, A., 2020. Attribution of ground-level ozone to anthropogenic and natural sources of nitrogen oxides and reactive carbon in a global chemical transport model. Atmos. Chem. Phys. 20, 10707–10731. https://doi.org/10.5194/acp-20-10707-2020.

Chang, K.-L., Petropavlovskikh, I., Cooper, O.R., Schultz, M.G., Wang, T., 2017. Regional trend analysis of surface ozone observations from monitoring networks in eastern North America, Europe and East Asia. Elementa-Sci. Anthrop. 5, 22. https://doi.org/10.1525/elementa.243.

Cooper, O.R., Schultz, M.G., Schroder, S., Chang, K.L., Gaudel, A., Benitez, G.C., Cuevas, E., Frohlich, M., Galbally, I.E., Molloy, S., Kubistin, D., Lu, X., McClure-Begley, A., Nedelec, P., O'Brien, J., Oltmans, S.J., Petropavlovskikh, I., Ries, L., Senik, I., Sjoberg, K., Solberg, S., Spain, G.T., Spangl, W., Steinbacher, M., Tarasick, D., Thouret, V., Xu, X., 2020. Multi-decadal surface ozone trends at globally distributed remote locations. Elementa-Sci. Anthrop. 8, 23. https://doi.org/10.1525/Elementa.420.

Emmons, L.K., Walters, S., Hess, P.G., Lamarque, J.-F., Pfister, G.G., Fillmore, D., Granier, C., Guenther, A., Kinnison, D., Laepple, T., Orlando, J., Tie, X., Tyndall, G., Wiedinmyer, C., Baughcum, S.L., Kloster, S., 2010. Description and evaluation of the model for ozone and related chemical tracers, version 4 (MOZART-4), geosci. Model Dev 3, 43–67. https://doi.org/10.5194/gmd-3-43-2010.

Emmons, L.K., Hess, P.G., Lamarque, J.-F., Pfister, G.G., 2012. Tagged ozone mechanism for MOZART-4, CAM-chem and other chemical transport models. Geosci. Model Dev. (GMD) 5, 1531–1542. https://doi.org/10.5194/gmd-5-1531-2012.

Fiore, A.M., Jacob, D.J., Bey, I., Yantosca, R.M., Field, B.D., Fusco, A.C., Wilkinson, J.G., 2002. Background ozone over the United States in summer: origin, trend, and contribution to pollution episodes. J. Geophys. Res. 107, 1–25. https://doi.org/10.1029/2001JD000982.

Fiore, A.M., Dentener, F.J., Wild, O., Cuvelier, C., Schultz, M.G., Hess, P., Textor, C., Schulz, M., Doherty, R.M., Horowitz, L.W., MacKenzie, I.A., Sanderson, M.G., Shindell, D.T., Stevenson, D.S., Szopa, S., Van Dingenen, R., Zeng, G., Atherton, C., Bergmann, D., Bey, I., Carmichael, G., Collins, W.J., Duncan, B.N., Faluvegi, G., Folberth, G., Gauss, M., Gong, S., Hauglustaine, D., Holloway, T., Isaksen, I.S.A., Jacob, D.J., Jonson, J.E., Kaminski, J.W., Keating, T.J., Lupu, A., Marmer, E., Montanaro, V., Park, R.J., Pitari, G., Pringle, K.J., Pyle, J.A., Schroeder, S., Vivanco, M.G., Wind, P., Wojcik, G., Wu, S., Zuber, A., 2009. Multimodel estimates of intercontinental source-receptor relationships for ozone pollution. J. Geophys. Res. 114, D04301 https://doi.org/10.1029/2008JD010816.

Gaudel, A., Cooper, O.R., Ancellet, G., Barret, B., Boynard, A., Burrows, J.P., Clerbaux, C., Coheur, P.F., Cuesta, J., Cuevas, E., Doniki, S., Dufour, G., Ebojie, F., Foret, G., Garcia, O., Granados-Munoz, M.J., Hannigan, J.W., Hase, F., Hassler, B., Huang, G., Hurtmans, D., Jaffe, D., Jones, N., Kalabokas, P., Kerridge, B., Kulawik, S., Latter, B., Leblanc, T., Le Flochmoen, E., Lin, W., Liu, J., Liu, X., Mahieu, E., McClure-Begley, A., Neu, J.L., Osman, M., Palm, M., Petetin, H., Petropavlovskikh, I., Querel, R., Rahpoe, N., Rozanov, A., Schultz, M.G., Schwab, J., Siddans, R., Smale, D., Steinbacher, M., Tanimoto, H., Tarasick, D.W., Thouret, V., Thompson, A.M., Trickl, T., Weatherhead, E., Wespes, C., Worden, H.M., Vigouroux, C., Xu, X., Zeng, G., Ziemke, J., 2018. Tropospheric Ozone Assessment Report: present-day distribution and trends of tropospheric ozone relevant to climate and global atmospheric chemistry model evaluation. Elementa-Sci. Anthrop. 6, 39. https://doi.org/10.1525/elementa.291.

Gaudel, A., Cooper, O.R., Chang, K.-L., Bourgeois, I., Ziemke, J.R., Stode, S.A., Oman, L. D., Sellitto, P., Nédélec, P., Blot, R., Thouret, V., Granier, C., 2020. Aircraft observations since the 1990s reveal increases of tropospheric ozone at multiple locations across the Northern Hemisphere. Sci. Adv. 6, eaba8272 https://doi.org/10.1126/sciadv.aba8272.

Gelaro, R., McCarty, W., Suárez, M.J., Todling, R., Molod, A., Takacs, L., Randles, C.A., Darmenov, A., Bosilovich, M.G., Reichle, R., Wargan, K., 2017. The modern-era retrospective analysis for Research and applications, version 2 (MERRA-2). J. Clim. 30, 5419–5454. https://doi.org/10.1175/JCLI-D-16-0758.1.

Georgoulias, A.K., van der A, R.J., Stammes, P., Boersma, K.F., Eskes, H.J., 2019. Trends and trend reversal detection in 2 decades of tropospheric NO2 satellite observations. Atmos. Chem. Phys. 19, 6269–6294. https://doi.org/10.5194/acp-19-6269-2019.

Grewe, V., Tsati, E., Mertens, M., Frömming, C., Jöckel, P., 2017. Contribution of emissions to concentrations: the TAGGING 1.0 submodel based on the modular Earth submodel System (MESSy 2.52). Geosci. Model Dev. (GMD) 10, 2615–2633. https://doi.org/10.5194/gmd-10-2615-2017.

Guerova, G., Bey, I., Attié, J.-L., Martin, R.V., Cui, J., Sprenger, M., 2006. Impact of transatlantic transport episodes on summertime ozone in Europe. Atmos. Chem. Phys. 6 https://doi.org/10.5194/acp-6-2057-2006, 2057–2072.

Guo, Y., Liu, J., Mauzerall, D.L., Li, X., Horowitz, L.W., Tao, W., Tao, S., 2017. Long-lived species enhance summertime attribution of North American ozone to upwind sources. Environ. Sci. Technol. 51, 5017–5025. https://doi.org/10.1021/acs.est.6b05664.

Hoesly, R.M., Smith, S.J., Feng, L., Klimont, Z., Janssens-Maenhout, G., Pitkanen, T., Seibert, J.J., Vu, L., Andres, R.J., Bolt, R.M., Bond, T.C., Dawidowski, L., Kholod, N., Kurokawa, J.-I., Li, M., Liu, L., Lu, Z., Moura, M.C.P., O'Rourke, P.R., Zhang, Q., 2018. Historical (1750–2014) anthropogenic emissions of reactive gases and aerosols from the community emissions data System (CEDS), geosci. Model Dev 11, 369–408. https://doi.org/10.5194/gmd-11-369-2018.

Jacob, D.J., Logan, J.A., Murti, P.P., 1999. Effect of rising Asian emissions on surface ozone in the United States. Geophys. Res. Lett. 26, 2175–2178. https://doi.org/10.1029/1999GL900450.

Kurokawa, J., Ohara, T., Morikawa, T., Hanayama, S., Janssens-Maenhout, G., Fukui, T., Kawashima, K., Akimoto, H., 2013. Emissions of air pollutants and greenhouse gases over Asian regions during 2000–2008: regional Emission inventory in ASia (REAS) version 2. Atmos. Chem. Phys. 13, 11019–11058. https://doi.org/10.5194/acp-13-11019-2013.

Lamarque, J.-F., Emmons, L.K., Hess, P.G., Kinnison, D.E., Tilmes, S., Vitt, F., Heald, C.L., Holland, E.A., Lauritzen, P.H., Neu, J., Orlando, J.J., Rasch, P.J., Tyndall, G.K., 2012. CAM-chem: description and evaluation of interactive atmospheric chemistry in the Community Earth System Model. Geosci. Model Dev. (GMD) 5, 369–411. https://doi.org/10.5194/gmd-5-369-2012.

Lu, X., Zhang, L., Wang, X., Gao, M., Li, K., Zhang, Y., Yue, X., Zhang, Y., 2020. Rapid increases in warm-season surface ozone and resulting health impact in China since 2013. Environ. Sci. Technol. Lett. 7, 240–247. https://doi.org/10.1021/acs.estlett.0c00171.

O'Neill, B.C., Tebaldi, C., van Vuuren, D.P., Eyring, V., Friedlingstein, P., Hurtt, G., Knutti, R., Kriegler, E., Lamarque, J.-F., Lowe, J., Meehl, G.A., Moss, R., Riahi, K., Sanderson, B.M., 2016. The scenario model Intercomparison Project (ScenarioMIP) for CMIP6, geosci. Model Dev 9, 3461–3482. https://doi.org/10.5194/gmd-9-3461-2016.

Price, C., Penner, J., Prather, M., 1997. NOx from lightning. 1. Global distribution based on lightning physics. J. Geophys. Res. 102, 5929–5941. https://doi.org/10.1029/96JD03504.

Ren, L., Yang, Y., Wang, H., Zhang, R., Wang, P., Liao, H., 2020. Source attribution of Arctic black carbon and sulfate aerosols and associated Arctic surface warming during 1980–2018. Atmos. Chem. Phys. 20, 9067–9085. https://doi.org/10.5194/acp-20-9067-2020.

Ren, L., Yang, Y., Wang, H., Wang, P., Chen, L., Zhu, J., Liao, H., 2021. Aerosol transport pathways and source attribution in China during the COVID-19 outbreak. Atmos. Chem. Phys. 21, 15431–15445. https://doi.org/10.5194/acp-21-15431-2021.

Schultz, M.G., Schröder, S., Lyapina, O., Cooper, O.R., Galbally, I., Petropavlovskikh, I., Von Schneidemesser, E., Tanimoto, H., Elshorbany, Y., Naja, M., Seguel, R.J., Dauert, U., Eckhardt, P., Feigenspahn, S., Fiebig, M., Hjellbrekke, A.-G., Hong, Y.-D., Kjeld, P.C., Koide, H., Lear, G., Tarasick, D., Ueno, M., Wallasch, M., Baumgardner, D., Chuang, M.-T., Gillett, R., Lee, M., Molloy, S., Moolla, R., Wang, T., Sharps, K., Adame, J.A., Ancellet, G., Apadula, F., Artaxo, P., Barlasina, M. E., Bogucka, M., Bonasoni, P., Chang, L., Colomb, A., Cuevas-Agullo, E., Cupeiro, M., Degorska, A., Ding, A., Fröhlich, M., Frolova, M., Gadhavi, H., Gheusi, F., Gilge, S., Gonzalez, M.Y., Gros, V., Hamad, S.H., Helmig, D., Henriques, D., Hermansen, O., Holla, R., Huber, J., Im, U., Jaffe, D.A., Komala, N., Kubistin, D., Lam, K.-S., Laurila, T., Lee, H., Levy, I., Mazzoleni, C., Mazzoleni, L.R., McClure-Begley, A., Mohamad, M., Murovec, M., Navarro-Comas, M., Nicodim, F., Parrish, D., Read, K. A., Reid, N., Ries, L., Saxena, P., Schwab, J.J., Scorgie, Y., Senik, I., Simmonds, P., Sinha, V., Skorokhod, A.I., Spain, G., Spangl, W., Spoor, R., Springston, S.R., Steer, K., Steinbacher, M., Suharguniyawan, E., Torre, P., Trickl, T., Lin, W., Weller, R., Xu, X., Xue, L., Ma, Z., 2017. Tropospheric ozone assessment Report: database and metrics data of global surface ozone observations. Elem. Sci. Anth. 5, 58. https://doi.org/10.1525/elementa.244.

Sicard, P., Paoletti, E., Agathokleous, E., Araminiene, V., Proietti, C., Coulibaly, F., De Marco, A., 2020. Ozone weekend effect in cities: deep insights for urban air pollution control. Environ. Res. 191, 110193 https://doi.org/10.1016/j.envres.2020.110193.

Sitch, S., Cox, P.M., Collins, W.J., Huntingford, C., 2007. Indirect radiative forcing of climate change through ozone effects on the land-carbon sink. Nature 448, 791–794. https://doi.org/10.1038/nature06059.

Sudo, K., Akimoto, H., 2007. Global source attribution of tropospheric ozone: long-range transport from various source regions. J. Geophys. Res. 112, D12302 https://doi.org/10.1029/2006JD007992.

Szopa, S., Naik, V., Adhikary, B., Artaxo, P., Berntsen, T., Collins, W.D., Fuzzi, S., Gallardo, L., Kiendler-Scharr, A., Klimont, Z., Liao, H., Unger, N., Zanis, P., 2021. Short-lived climate forcers. In: Masson-Delmotte, V., Zhai, P., Pirani, A., Connors, S. L., Péan, C., Berger, S., Caud, N., Chen, Y., Goldfarb, L., Gomis, M.I., Huang, M., Leitzell, K., Lonnoy, E., Matthews, J.B.R., Maycock, T.K., Waterfield, T., Yelekçi, O., Yu, R., Zhou, B. (Eds.), Climate Change 2021: the Physical Science Basis. Contribution of Working Group I to the Sixth Assessment Report of the

Intergovernmental Panel on Climate Change. Cambridge University Press, Cambridge, United Kingdom and New York, NY, USA, pp. 817–922. https://doi.org/10.1017/9781009157896.008.

Tilmes, S., Lamarque, J.-F., Emmons, L.K., Kinnison, D.E., Ma, P.-L., Liu, X., Ghan, S., Bardeen, C., Arnold, S., Deeter, M., Vitt, F., Ryerson, T., Elkins, J.W., Moore, F., Spackman, J.R., Val Martin, M., 2015. Description and evaluation of tropospheric chemistry and aerosols in the community Earth System model (CESM1.2). Geosci. Model Dev. (GMD) 8, 1395–1426. https://doi.org/10.5194/gmd-8-1395-2015.

van Marle, M.J.E., Kloster, S., Magi, B.I., Marlon, J.R., Daniau, A.-L., Field, R.D., Arneth, A., Forrest, M., Hantson, S., Kehrwald, N.M., Knorr, W., Lasslop, G., Li, F., Mangeon, S., Yue, C., Kaiser, J.W., van der Werf, G.R., 2017. Historic global biomass burning emissions for CMIP6 (BB4CMIP) based on merging satellite observations with proxies and fire models (1750–2015). Geosci. Model Dev. (GMD) 10, 3329–3357. https://doi.org/10.5194/gmd-10-3329-2017.

Wang, X., Fu, T.-M., Zhang, L., Lu, X., Liu, X., Amnuaylojaroen, T., Latif, M.T., Ma, Y., Zhang, L., Feng, X., Zhu, L., Shen, H., Yang, X., 2022. Rapidly changing emissions drove substantial surface and tropospheric ozone increases over Southeast Asia. Geophys. Res. Lett. 49, e2022GL100223 https://doi.org/10.1029/2022GL100223.

Yang, Y., Wang, H., Smith, S.J., Ma, P.-L., Rasch, P.J., 2017. Source attribution of black carbon and its direct radiative forcing in China. Atmos. Chem. Phys. 17, 4319–4336. https://doi.org/10.5194/acp-17-4319-2017.

Yang, Y., Wang, H., Smith, S.J., Zhang, R., Lou, S., Yu, H., Li, C., Rasch, P.J., 2018. Source apportionments of aerosols and their direct radiative forcing and long-term trends over continental United States. Earth's Future 6, 793–808. https://doi.org/10.1029/2018EF000859.

Yang, Y., Zhou, Y., Li, K., Wang, H., Ren, L., Zeng, L., Li, H., Wang, P., Li, B., Liao, H., 2021. Atmospheric circulation patterns conducive to severe haze in eastern China have shifted under climate change. Geophys. Res. Lett. 48, e2021GL095011 https://doi.org/10.1029/2021GL095011.

Zhang, Y., Cooper, O.R., Gaudel, A., Thompson, A.M., Nedelec, P., Ogino, S.-Y., West, J. J., 2016. Tropospheric ozone change from 1980 to 2010 dominated by equatorward re-distribution of emissions. Nat. Geosci. 9, 875–879. https://doi.org/10.1038/NGEO2827.

Zhang, J.J., Wei, Y., Fang, Z., 2019. Ozone pollution: a major health hazard worldwide. Front. Immunol. 10, 2518. https://doi.org/10.3389/fimmu.2019.02518.

Zhang, Y., West, J.J., Emmons, L.K., Flemming, J., Jonson, J.E., Lund, M.T., Sekiya, T., Sudo, K., Gaudel, A., Chang, K.-L., Nédélec, P., Thouret, V., 2021. Contributions of world regions to the global tropospheric ozone burden change from 1980 to 2010. Geophys. Res. Lett. 48, e2020GL089184 https://doi.org/10.1029/2020GL089184.

Zheng, B., Tong, D., Li, M., Liu, F., Hong, C., Geng, G., Li, H., Li, X., Peng, L., Qi, J., Yan, L., Zhang, Y., Zhao, H., Zheng, Y., He, K., Zhang, Q., 2018. Trends in China's anthropogenic emissions since 2010 as the consequence of clean air actions. Atmos. Chem. Phys. 18, 14095–14111. https://doi.org/10.5194/acp-18-14095-2018.

Ziemke, J.R., Oman, L.D., Strode, S.A., Douglass, A.R., Olsen, M.A., McPeters, R.D., Bhartia, P.K., Froidevaux, L., Labow, G.J., Witte, J.C., Thompson, A.M., Haffner, D. P., Kramarova, N.A., Frith, S.M., Huang, L.-K., Jaross, G.R., Seftor, C.J., Deland, M. T., Taylor, S.L., 2019. Trends in global tropospheric ozone inferred from a composite record of TOMS/OMI/MLS/OMPS satellite measurements and the MERRA-2 GMI simulation. Atmos. Chem. Phys. 19, 3257–3269. https://doi.org/10.5194/acp-19-3257-2019.